



# SPACE TRUSSES AS IMPACT ENERGY ABSORBERS: AN EXPERIMENTAL STUDY

**Abdulmalik Ali Aljinaidi Alghamdi<sup>1</sup>**

*1: Associate Professor, Department of Mechanical Engineering, King Abdulaziz University*

*PO Box 80204, Jeddah 21589, Saudi Arabia*

*Fax: 966-2-695-2193, E-mail: aljinaidi@hotmail.com*

## **ABSTRACT**

*This study explores the performance of space trusses when used as impact energy absorbers. Space trusses exist as structural elements in civilian and military establishments. This paper reviews the most common shapes of collapsible energy absorbers and highlights the different modes of deformation of thin tubes. Experimental study includes crushing of 27 low-carbon steel space trusses of different diameters and different aspect ratios between two rigid parallel plates at quasi-static loading condition. Obtained results illustrate the deformation mode of the space trusses and highlight the relatively low efficiency of the absorber.*

**Keywords:** *Energy Absorber, Impact Mechanics*

## **1. INTRODUCTION**

Functions of structural elements need to be redefined to include the safe design of members to withstand impact forces during crash events in an attempt to minimize human losses. Thus, efforts need to be made to understand the behavior of common shapes of structures under impact loading and large deformation.

Impact studies in the vehicle industry are well known and well developed [Averill et al. 2001]. However, it is becoming apparent that, in the future, other fields of industry need to look at their structural elements from energy absorption consideration [Valenti, 1999]. The current trend in producing lighter structures, like plastics and fiberglass composites, puts greater

demands on the designer to avoid working in the elastic zone alone and ignoring the plastic behavior of the structure under large displacement. Thus, with the advances in composite materials it is expected that results of composite crashworthiness research will lead to absorbers with variable directional energy absorption.

## **2. ENERGY ABSORBERS**

Impact engineering has been a hot subject in the second half of the last century. Efforts have been made towards better understanding of failure modes and energy dissipation patterns during impact in common structures. The common objective of researchers is to build safer structures and evaluate existing ones from energy absorption point of view in order to reduce losses in human and material resources in crash events. Application of impact engineering includes areas such as aircraft crashworthiness, nuclear reactor safety, crash barrier design, offshore structures, oil tankers [Valenti, 1999] and collision damage to road bridges [Alghamdi, 2000].

### **2.1 Definition**

An energy absorber is a system that converts, totally or partially, kinetic energy into another form of energy. Energy converted is either reversible, like pressure energy in compressible fluids and elastic strain energy in solids, or irreversible, like plastic deformation energy [Alghamdi, 2001a].

The designer of the collapsible impact energy absorber is required to come up with a system of thin structure that absorbs the majority of the kinetic energy of moving bodies within the system itself in an irreversible manner. The selection of the proper absorber depends on factors such as material properties, absorber shape, absorber structural inertia, loading rate and allowable displacement patterns [Johnson and Reid, 1978].

Deformable energy absorbers include items such as steel drums [Carney and Pothen, 1988], three-dimensional tubular cells [Alghamdi, 2001b], circular tubes [Alexander, 1960], two-dimensional tubular rings [Reid et al., 1984], square tubes [Nannucci et al. 1999], frusta [Alghamdi, et al. 2001], corrugated tubes [Singace and El-Sobky, 1997], and sandwich plates [Corbett and Reid, 1993]

Thin tubes can be deformed in different modes of deformation such as axial crushing [Alexander, 1960], tube inversion [Al-Hassani et al., 1972], lateral indentation [Watson et al., 1976], lateral crushing [Johnson, et al. 1977], tube splitting [Stronge et al., 1984] and tube nosing [Reid and Harrigan, 1998]. Also, thin circular tubes have been tested when filled with foam [Nahas, 1993] and wood [Reddy and Al-Hassani, 1993].

### 3. ABSORBER SHAPE

Researchers have suggested absorbers with different shapes since the pioneering work of Alexander in early 1960s. Common proposed shapes are listed below:

- a. **Cubic rod cell** made of 12 low carbon steel rods welded together, see Alghamdi, (2000).
- b. **Frusta** (truncated circular cones) that have wide ranges of applications in the field of armament and military industries, see Alghamdi, (1991).
- c. **Multicorner Columns** such as square tubes and honeycomb cells, see Wu and Jiang (1997).
- d. **Polygonal cross-section cylinders** subjected to axial loading, see Mamalis et al., (1991a).
- e. **Three-dimensional tubular cell** made of 12 thin tubes welded together to form a cubic cell, see Alghamdi, (2001).
- f. **Tubes** represent the most common shape of collapsible impact energy absorbers, because of their high frequency of occurrence as structural elements, see Reid, (1993).
- g. **Sandwich plates** especially in the transportation industry, see Worrall (1990).
- h. **Single-hat** thin walled sections, see White and Jones, (1999).
- i. **Spherical shells** under axial crushing between rigid plates, see Gupta et al., (1999).
- j. **Struts** such as road guardrail terminals, see Reid and Sicking (1998).
- k. **W-structure** made of 4 rods connected by 3 elbows, see Johnson and Reid, (1978).

### 4. THE PROPOSED SYSTEM

Each absorber has its own characteristics under impulsive loading. The deformation pattern is extremely complex and the degree of complexity increases as the shape becomes more complex. The study of plastic deformation in energy absorbers accounts for geometrical changes, such as tube diameter, for axially loaded tubes, and interaction between various modes of deformation as well as strain hardening and strain rate effects.

In this paper the energy absorption of a common structural member is being introduced and investigated experimentally. The proposed shape is a tetrahedron space truss made of six identical solid low-carbon steel rods welded together, see Figure 1. Space trusses can be found in different applications including: 1) Space stations, 2) satellites, 3) armory applications and 4) civilian application in structural industry especially in bridges.

The aim of this paper is to investigate the crushing behavior of the space truss under static loading case. This includes:

- a. Studying the effect of rod diameter on the absorbed energy
- b. Studying the effect of aspect ratio (space truss length/space truss diameter) on the absorbed energy
- c. Determining the energy density per unit mass of the absorber
- d. Predicting an empirical average crushing force in terms of the system physical properties such as yield strength and basic geometries like rod diameter.

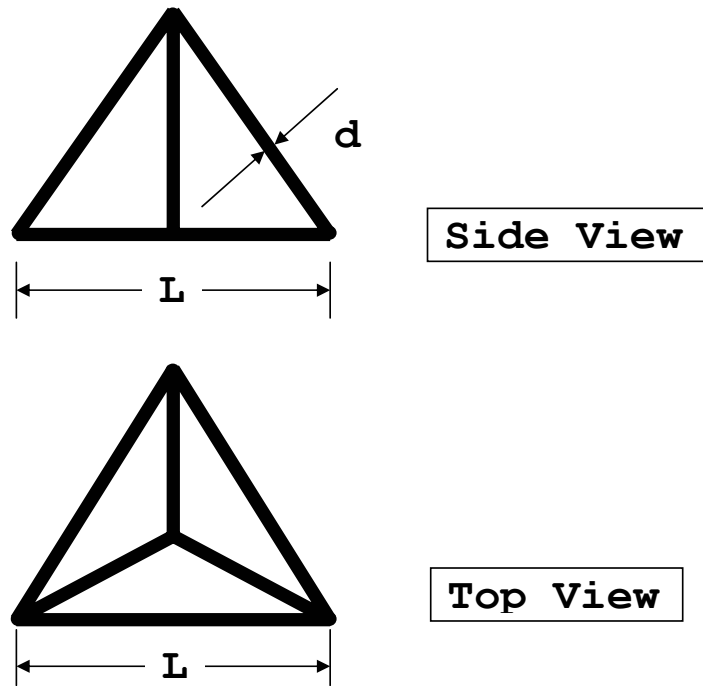


Figure 1: Schematic Drawing of the Space Truss.

## 5. EXPERIMENTAL WORK

Twenty-seven absorbers made of low-carbon steel rods with yield strength  $S_y = 250$  MPa were manufactured by arc welding. Table 1 lists the dimensions of these absorbers. These absorbers are grouped into three different rod diameters (6mm, 8mm, 10mm) and eight aspect ratios (8 to 22). Aspect ratio (R) is defined as the ratio between rod length (L) and rod diameter (d). The experimental program is conducted by crushing these absorbers using 10-Ton Universal Instron Machine and a crushing rate of 5 mm/min is maintained throughout

Table 1: Dimensions of the Specimens Used and Details of the Experimental Program.

No.	Sp. No.	d (mm)	L (mm)	R=L/d	m (g)	F <sub>max</sub> (N)	F <sub>av</sub> (N)	E (J)	E* (J/g)	Remarks
1	608	6	48	8	63	24820	17800	391.7	6.217	Sym. Deformation, Small Shift, No Rotation
2	610	6	60	10	73	23740	15100	377.6	5.172	Sym. Deformation, No Shift, Small Rotation
3	612	6	72	12	92	23750	11600	359.5	3.907	Nonsym. Def., Large Shift, One Leg Rotation, SS
4	614	6	84	14	105	21780	8648	389.2	3.706	Nonsym. Deformation, Large Shift, One Leg Rotation, SS
5	616	6	96	16	122	24330	8233	510.5	4.184	Nonsym. Def., Large Shift, Two Leg Rotation, SS
6	618	6	108	18	139	19130	10380	726.3	5.225	Sym. Deformation, Small Shift, Three Leg Rotation, SS
7	620	6	120	20	156	18200	7207	180.1	1.155	Stopped After 25 mm
8	622	6	132	22	177	17410	6650	166.3	0.9393	Stopped After 25 mm
9	808	8	64	8	135	38260	30570	856.0	6.340	Sym. Def., No Shift, No Rotation, Secondary Sup. (SS)
10	810	8	80	10	173	39740	24587	909.7	5.259	Sym. Def., No Shift, No Rotation, Secondary Sup. (SS)
11	812	8	96	12	213	41010	24340	1461	6.858	Sym. Deformation, No Shift, Small Rotation, SS
12	814	8	112	14	252	38850	23551	1507	5.981	Sym. Deformation, Large Shift, Three Leg Rotation, SS
13	816	8	128	16	288	38460	18290	1555	5.399	Sym. Deformation, Small Shift, Three Leg Rotation, SS
14	818	8	144	18	331	35510	15730	550.5	1.663	Stopped After 38 mm
15	820	8	160	20	367	32370	13740	412.1	1.123	Stopped After 34 mm
16	822	8	176	22	400	31050	12410	372.4	0.9311	Stopped After 32 mm
17	1006	10	60	6	222	74750	60120	990	4.460	Sym. Deformation, No Shift, No Rotation, Weld Brake
18	1007	10	70	7	254	64350	36090	1444	5.683	Nonsym. Def., Large Shift, No Rotation, Weld Brake
19	1009	10	90	9	327	64700	39710	2184	6.679	Sym. Def., Small Shift, No Rotation, Weld Brake, SS
20	1010	10	100	10	370	66060	35340	1750	4.731	Nonsym. Def., Small Shift, Small Rotation, Weld Brake
21	1011	10	110	11	405	65040	33430	2675	6.604	Sym. Deformation, Small Shift, No Rotation, SS
22	1013	10	130	13	466	66510	31310	626.3	1.344	Stopped After 21 mm
23	1014	10	140	14	518	57610	25050	1750	3.379	Nonsym. Def., Large Shift, 3 Leg Rotation, Weld Brake
24	1015	10	150	15	539	61800	23740	1068	1.982	Stopped After 46 mm
25	1017	10	170	17	628	55720	19070	1335	2.126	Stopped After 70 mm
26	1019	10	190	19	707	55030	20600	824.0	1.165	Stopped After 40 mm
27	1021	10	210	21	766	49340	19190	1919	2.505	Stopped After 100 mm

the tests. Obtained experimental results are summarized in Table 1 and discussed in details in the following section. Table 1 contains mass ( $m$ ) of each space truss, energy ( $E$ ) absorbed during crushing and specific energy ( $E^*$ ) predicted by dividing the absorbed energy by the mass of the absorber.

## 6. RESULTS AND DISCUSSIONS

As stated above, the main objective of this paper is to elaborate the crushing behavior of space trusses under static loading condition. Typical load-displacement curve is shown in Figure 2 for Specimen 812, see Table 1. The rod diameter of the specimen is 8 mm, aspect ratio is 12 and its mass is 213 g. The load increases from zero to a maximum value. The recorded maximum peak force ( $F_{max}$ ) at point a in Figure 2 is 41010 N. This point represents the maximum instability (resistance) value where the absorber starts crumpling after this point. The plastic deformation starts before point “a” and continues after ward. The load decreases between point a and point b which represents the global minimum in the curve. At point “a” a line is drawn to represent a leg of the truss. Then as the deformation progresses from point a to point b, the straight-line bend plastically (permanently) at a plastic hinge located in the middle of the rod. The direction of deformation is outward for all trusses tested, i.e., each rod undergoes counterclockwise rotation at the plastic hinge. The decrease in the load between points a and b is attributed to the increase of the bending arm for constant plastic moment. Two different frames given in the figure simplify the behavior of the rod. Note that the three rods in the base of the truss undergo no bending or stretching work. More or less, in some cases they are exposed to twisting work coming from the boundary. Yet, they are necessary to hold the space truss as well. At point b the upper part of the leg becomes almost straight and the lower one touches the upper plate. This is considered as a secondary support and hence a sudden increase in the load. The load increases from point b to point c, which represents another instability value, and then decreases due to the increase in the bending arm in the second stage of crumpling as shown in the schematic drawing. The second crumpling takes fewer wavelengths when compared to the first one. At point d the space truss becomes flat and beyond point d the deformation is changed from crumpling to direct compression. Looking to the load-displacement curve shown in Figure 2 one can see the “duck shape”. In some cases legs rotate in the horizontal plane (base plane) during crushing.

For ideal space truss with no imperfection, the deformation pattern is repeated in fluctuation pattern with shorter wavelength as the crumpling continues. Figure 3 illustrates the load-displacement curves for absorbers with different aspect ratios ( $R=8, 10, 14$  and  $16$ ), and same rod diameter ( $d=8$  mm). For the top two curves ( $R=8$  and  $R=10$ ) space trusses were short to form a secondary crumpling and the shown increase in the load is due to the direct compression effect. As the aspect ratio is increased, the size of the absorber increases and hence one can see more than one crumpling. However, for absorber with large aspect ratio,

the crushing mode is changed into global unstable elastic mode in one bar with tendency to shift center of the absorber outside the base. Thus, experiments were stopped for trusses with large aspect ratios. One can see from the remarks written in Table 1 that as the aspect ratio increases, the deformation is changed from symmetric to nonsymmetric, center of the truss moves away from the center of the base and rotation of the vertical rods increases during crumpling.

The effect of increasing rod diameter on the load-displacement curve at constant aspect ratio is shown in Figure 4. As expected, the peak force increases with the increase in the rod diameter, but the shape of the curve is unchanged. There is only one outward crumpling because the space trusses are too short to allow a second one to exist.

The peak force is plotted versus aspect ratio for the different rod diameters in Figure 5. As expected, the instability force increases with the increase in rod diameter, at a step proportional to the change in cross sectional area of the rods. This shows consistency in the experiment with an acceptable level of variation. Also, the maximum force decreases with the increase in rod length as a result of aspect ratio increase.

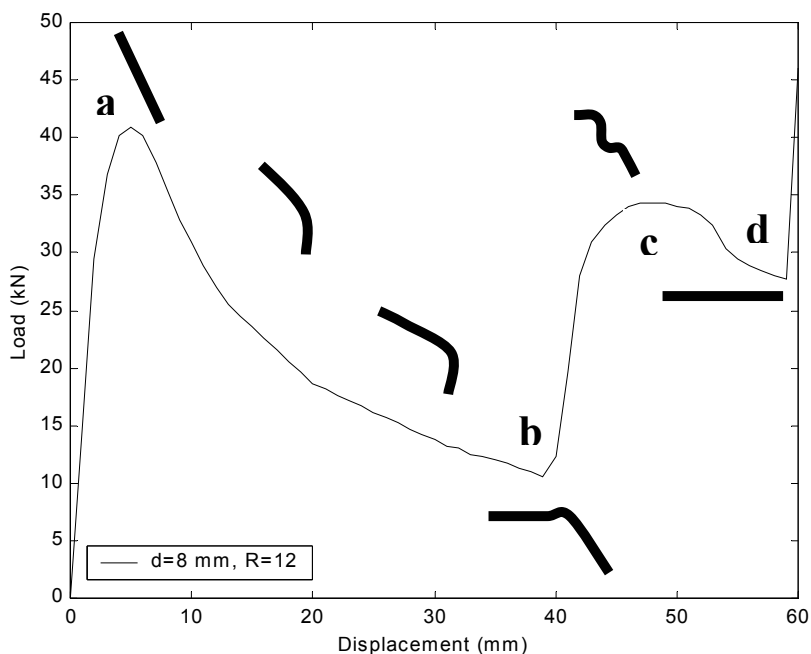


Figure 2: Load Displacement Curve for Specimen 812.

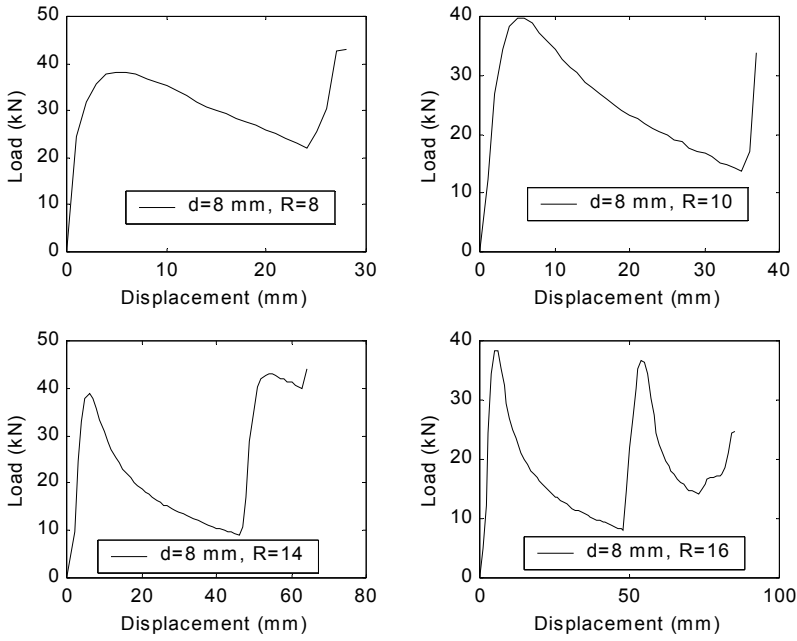


Figure 3: Load-Displacement Curves for Specimens 808, 810, 814 and 816.

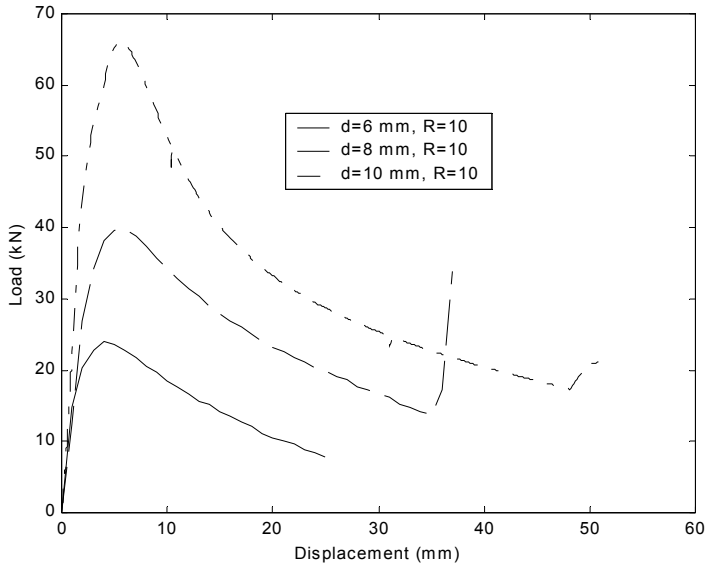


Figure 4: Load-Displacement Curves for Specimens 610, 810 and 1010.

Device efficiency represented by the specific energy or the energy absorbed per unit mass is shown in Figure 6. The specific energy is plotted verse the aspect ratio of all trusses tested in Table 1. This includes stopped tests that have low energy density. The first thing to notice is the low energy density of the proposed absorber that appears in one single digit. These values are considered low when compared to axial crushing of tubes with specific energy that can reach 30 J/g, [Reid, 1993]. Generally speaking the specific energy decreases with the increase in aspect ratio and attain maximum value in the neighborhood of R=9.

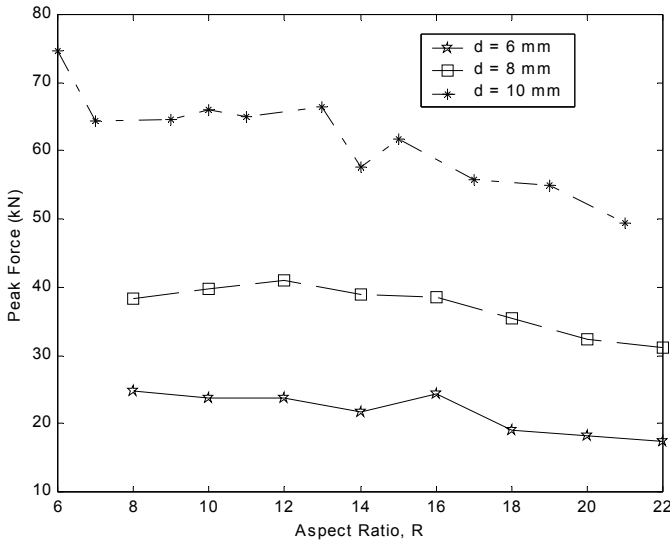


Figure 5: The Relationship Between Maximum Crushing Force and Aspect Ratio.

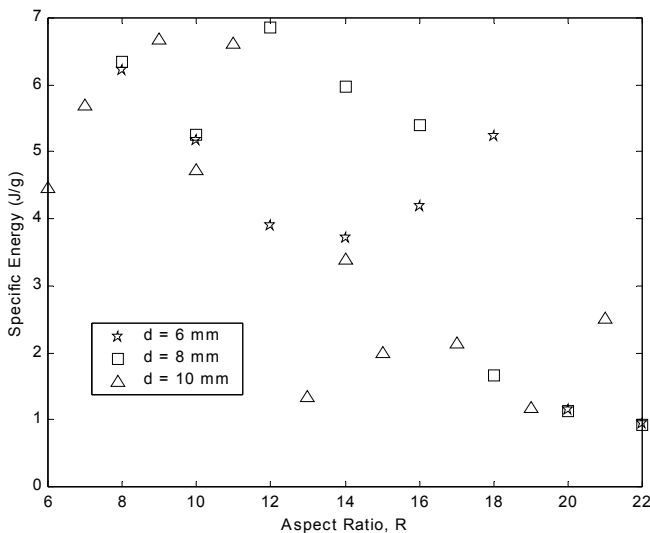


Figure 6: The Specific Energy vs. Aspect Ratio.

## 7. ANALYSIS

The experimental peak force given in Table 1 is supported by three legs (rods) in the space truss. The relation between the axial force at the top of the space truss (F) and the compression force (P) developed in each leg is given by

$$P = 0.408 F \quad (1)$$

Equation 1 assumed perfect shape with no imperfection and truss with hinged joints. Now this maximum compression force is related, for the sake of analysis, to the buckling load and the yielding load. When considering yielding load only cross sectional area and yield strength of the bar are considered. Thus the yielding force is independent of space truss length, i.e. aspect ratio. For long (Euler) column analysis, the boundary condition of the leg is assumed to be pinned-pinned condition, and the stability force depends on space truss length. The validity of Euler analysis is restricted by the critical slenderness ratio that is a material property. For short (Johnson) column analysis, length of the leg has less contribution when compared to Euler buckling load. Now, putting all of the analytical predictions and experimental tests together results in diagrams shown in Figures 7-9.

Legs of the space trusses tested in the experimental program are all short when comparing their slenderness ratios (effective length divided by radius of gyration) to the critical value, found to be 125 for the material used. Euler column prediction values were trim out for small aspect ratio in order to have a better look at these curves. It is found out that the experimental value for the peak force is bounded by the upper long-column curve and lower short-column curve. And for the tested range of aspect ratio, the lower bound is the yielding force as shown in all figures. Also, experimental peak forces approach the yielding forces with the increase in aspect ratio.

From buckling analysis point of view the yielding line should be the upper limit for the peak force, however, that is correct for one single leg or column pressed axially. Thus the integrity of the space truss increases the load carrying capacity of each member.

Average experimental crushing force per rod is plotted vs. aspect ratio in Figure 10 for the three diameters. Then empirical relation is fitted to these data. The best curve fit selected among several models [Bogis et al., 2001] is found to be in the form

$$F_{av} = \alpha A S_y / L \quad (2)$$

Where  $\alpha$  is a constant equals 8.1, A is the cross-sectional area of the rod,  $S_y$  is the yield strength and L is the rod length. As usual, application of Equation 2 is restricted to space trusses made of low carbon steel in the given range of diameters and aspect ratios.

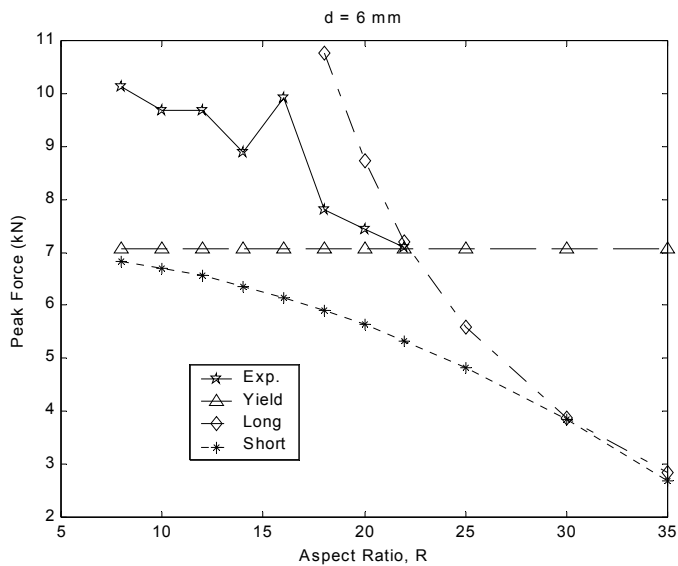


Figure 7: Experimental and Analytical Peak Forces vs. Aspect Ratio For d=6 mm.

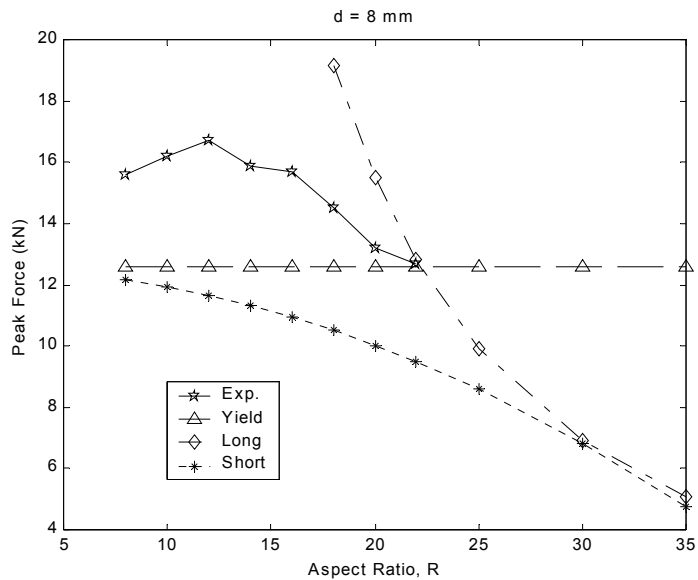


Figure 8: Experimental and Analytical Peak Forces vs. Aspect Ratio For d=8 mm.

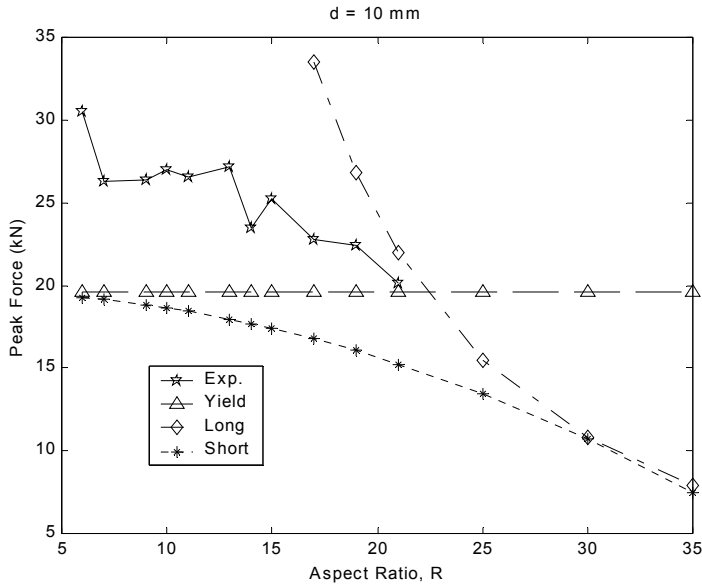


Figure 9: Experimental and Analytical Peak Forces vs. Aspect Ratio For d=10 mm.

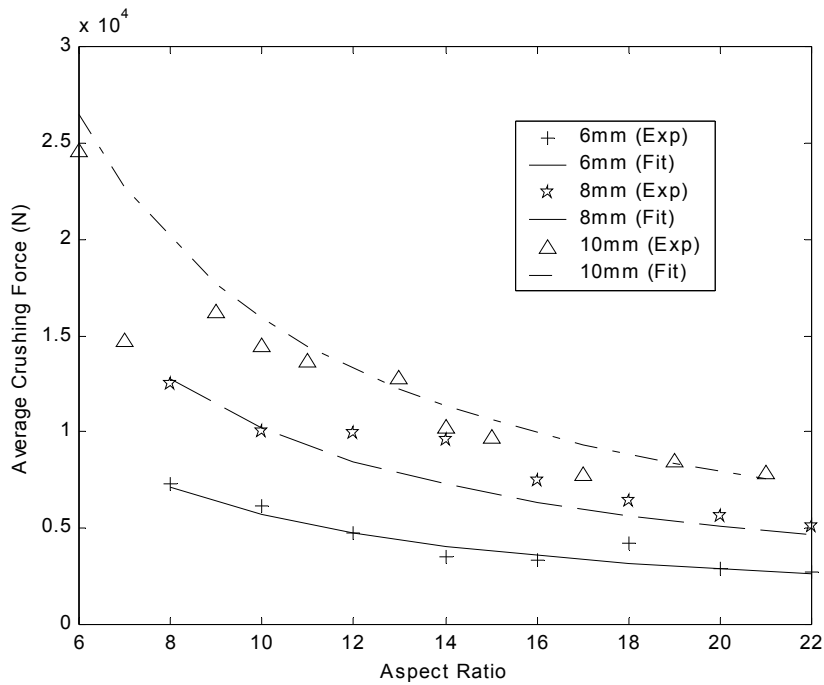


Figure 10: Experimental and Empirical Average Force vs. Aspect Ratio For d = 6, 8, and 10 mm.

## 8. CONCLUSIONS

This paper discusses the deformation pattern of space trusses when crushed between two parallel plates. The aim is to understand the response of space truss when forced to be used as impact energy absorber. It is found that, the absorber deforms in a predetermined pattern especially for compact ones with small aspect ratio. As expected, the obtained energy density is not high when compared to other thin structures like thin tubes due to the limited amount of material of the space truss participates in plastic deformation during crumpling. Plastic work is seen in the form of plastic bending of vertical rods and plastic twisting of both vertical and horizontal (base) rods.

## ACKNOWLEDGEMENT

The author would like to thank King Abdulaziz University for their support during his sabbatical leave during 2001/2002 academic year. Help provided by Khalid Badeghaish in specimens preparation is highly appreciate.

## REFERENCES

1. Alexander, J. M., 1960, "An Approximate Analysis of the Collapse of Thin Cylindrical Shells Under Axial Loading," *Quarterly Journal of Mechanics and Applied Mathematics*, 13 (1), pp. 10-15.
2. Alghamdi, A. A. A., 1991, "Design of Simple Collapsible Energy Absorber," *Master of Science Thesis*, College of Engineering, King Abdulaziz University, Jeddah, Saudi Arabia.
3. Alghamdi, A. A. A., 2000, "Protection of Saudi Descent Roads using Metallic Collapsible Energy Absorbers," Final Report Submitted to KACST, Riyadh, Saudi Arabia, Grant Number 98-2-74.
4. Alghamdi, A. A. A., 2001a, "Collapsible Energy Absorbers: An Overview," *Thin-Walled Structures*, 39, pp. 189-213.
5. Alghamdi, A. A. A., 2001b, "Three Dimensional Tubular Impact Energy Absorber", *European Journal of Mechanical and Environmental Engineering*, Submitted.
6. Alghamdi, A. A. A., Aljawi, A. A. N. and Abu-Mansour, T. M. N., 2001, "Modes of Axial Collapse of Unconstrained Capped Frusta," *International Journal of Mechanical Engineering*, Accepted.
7. Al-Hassani, S. T. S., Johnson, W. and Lowe, W. T., 1972, "Characteristics of Inversion Tube Under Axial Loading," *Journal of Mechanical Engineering Science*, 14, pp. 370-381.
8. Averill, R., Eby, D. and Goodman, E., 2001, "How Well Can It Take a Hit," *Mechanical Engineering Design Magazine*, pp. 26-28.
9. Bogis, H. A., Abou Ezz, A., Akyurt, M. and Alghamdi, A. A. A., 2001, "An Interactive Software for Curve Fitting," *International Journal of Mechanical Engineering Education*, Submitted.

10. Carney III, J. F. and Pothen, S., 1988, "Energy Dissipation in Braced Cylindrical Shells," *International Journal of Mechanical Science*, 30 (3/4), pp. 203-216.
11. Corbett, G. G. and Reid, S. R., 1993, "Local Loading of Simply-Supported Steel-Grout Sandwich Plates," *International Journal of Impact Engineering*, 13 (3), pp. 443-461.
12. Gupta, N. K., Prasad, G. L. Gupta, S. K., 1999, "Axial Compression of metallic Spherical Shells between Rigid Plates," *Thin-Walled Structures*, 34 (1), pp. 21-41.
13. Johnson, W. and Reid, S. R., 1978, "Metallic Energy Dissipating Systems," *Applied Mechanics Review*, 31 (3), pp. 277-288.
14. Johnson, W., Reid, S. R. and Reddy, T. Y., 1977, "The Compression of Crossed Layers of Thin Tubes," *International Journal of Mechanical Science*, 19, pp. 423-437.
15. Mamalis, A. G., Manolakos, D. E., Baldoukas, A. K. and Viegelaahn, G., 1991, "Energy Dissipation and Associated Failure Modes when Axially Loading Polygonal Thin-Walled Cylinders," *Thin-Walled Structures*, 12 (1), pp. 17-34.
16. Nahas, M. N., 1993, "Impact Energy Dissipation Characteristics of Thin-Walled Cylinders," *Thin-Walled Structures*, 15 (2), pp. 81-93.
17. Nannucci, P. R., Marshall, N. S. and Nurick, G. N., 1999, "A Computational Investigation of the Progressive Buckling of Square Tubes with Geometric Imperfections," *3<sup>rd</sup> Asia-Pacific Conference on Shock and Impact Loads on Structures*, Singapore.
18. Reddy, T. Y. and Al-Hassani, S. T. S., 1993, "Axial Crushing of Wood-Filled Square Metal Tubes," *International Journal of Mechanical Science*, 35 (3/4), pp. 231-246.
19. Reid, S. R., 1993, "Plastic Deformation Mechanisms in Axially Compressed Metal Tubes used as Impact Energy Absorbers," *International Journal of Mechanical Science*, 35 (12), pp. 1035-1052.
20. Reid, J. D. and Sicking, D. L., 1998, "Design and Simulation of a Sequential Kinking Guardrail Terminal," *International Journal of Impact Engineering*, 21 (9), pp. 761-772.
21. Reid, S. R., Austin, C. D. and Smith, R., 1984, "Tubular Rings as Impact Energy Absorber," In *Structural Impact and Crashworthiness*, Davies, G. and Morton, J.(Eds.), Elsevier, New York, pp. 555-563.
22. Reid, S. R. and Harrigan, J. J., 1998, "Transient Effects in the Quasi-Static and Dynamic Internal Inversion and Nosing of Metal Tubes," *International Journal of Mechanical Science*, 40 (2/3), pp. 263-280.
23. Singace, A. A. and El-Sobky, H., 1997, "Behaviour of Axially Crushed Corrugated Tubes," *International Journal of Mechanical Science*, 39 (3), pp. 249-268.
24. Stronge, W. J., Yu, T. X. and Johnson, W., 1984, "Long Stroke Energy Dissipation in Splitting Tubes," *International Journal of Mechanical Science*, 25 , pp. 637-647.
25. Valenti, M., 1991, "Double Wrapped," *Mechanical Engineering Magazine*, pp. 52-56, January.
26. Watson, A. R., Reid, S. R., Johnson, W. and Thomas, S. G., 1976, "Large Deformation of Thin-Walled Circular Tubes Under Transverse Loading," *International Journal of Mechanical Science*, 18 (5), pp. 387-396.

27. White, M. D. and Jones, N., 1999, "Experimental Quasi-Static Axial Crushing of Top-Hat and Double-Hat Thin-Walled Sections," *International Journal of Mechanical Science*, 41, pp. 179-208.
28. Worrall, C. M., 1990, "Behaviour of Composite Sandwich Beams and Panels under Low Velocity Impact Conditions," *Ph.D. Thesis*, University of Liverpool.
29. Wu, E. and Jiang, W-S., 1997, "Axial Crush of Metallic Honeycombs," *International Journal of Impact Engineering*, 19 (5/6), pp. 439-456.